COLOR HIT-OR-MISS TRANSFORM ($CMOMP$)

Audrey Ledoux, Noël Richard and Anne-Sophie Capelle-Laizé

University of Poitiers, XLIM-SIC JUR CNRS 7252, Poitiers, France
Telephone: +33 (0)5 49 49 74 92
Fax: +33 (0)5 49 49 65 70

ABSTRACT

Often, the mathematical morphology is reduced to the ordering construction and the structuring elements are limited to flat shapes. In this paper, we propose a new method based on concept of *convergence*. Within this proposition, the definition of non-flat structuring element is now possible. By extending the mathematical morphology hit-or-miss transform to the color, we show that these formalisms are well adapted for complex color images, as skin images for dermatological purposes. We give and comment results on synthetic and real images.

Index Terms— color mathematical morphology, non-flat structuring element, hit-or-miss

1. INTRODUCTION

The extension of Mathematical Morphology (MM) to color images is not straightforward, due to the complexity of vectorial data ordering. The abundance of color spaces [1] and possible color ordering methods [2] allow a near infinity of expressions for color MM. Some authors define a total order in multivariate values [3]. But none deals with the question of color Non-Flat Structuring Element ($NFSE$) that are used in some morphological operations in grayscale functions or images (filtering [4], estimation of the fractal dimension [5] ...). In this paper we propose a new color MM in the $CIELAB$ color space that permits the definition of non-flat structuring element. We evaluate this new method using the color Hit-or-Miss Transform (HMT) to extract complex color structures in natural images, like skin images.

The first part of this paper is a quick recall on the Hit-or-Miss Transform in binary and grayscale, with focus on the Barat's proposal [6] (section 2). Then, we present our color MM construction to obtain a total order allowing $NFSE$ writing (section 3). We explain how to solve questions about a valid construction of color addition/subtraction. Finally, we show results on synthetic images to evaluate the approach interest for color images (section 4) and we apply and validate this approach in our applicative context (section 5).

2. HIT-OR-MISS TRANSFORM

The Hit-or-Miss Transform (HMT) allows to find specific shapes in images. It was initially developed for binary images by Matheron and Serra [7]. The searched shapes are defined with a pair of disjoint Structuring Elements (SE) that frame it, one for the foreground shape and one for the background shape. The mathematical expression of the HMT for an image f and its structuring elements $g = \{g', g''\}$ is:

$$HMT_g(f)(x) = (f \ominus_{\mathfrak{b}} g')(x) \cap (f^c \ominus_{\mathfrak{b}} g'')(x) \quad (1)$$

where f^c is the complement of f, $f^c = \{x | x \notin f\}$.

Several variations exists around the definition in grayscale [8, 9, 10, 11]. In the following we explain the Barat proposal [6], called $MOMP$ (Multiple Objects Matching using Probing). The $MOMP$ transform is an image surface probing with two SEs, one above the surface (g'') and the second below (g'). The mathematical expression of the $MOMP$ is:

$$MOMP_g(f)(x) = (f \oplus_{\mathfrak{g}} (-g'')^r)(x) - (f \ominus_{\mathfrak{g}} g')(x) \quad (2)$$

Table 1: Notations

$f, \mathcal{D}_f$	Image function and his spatial domain of definition
$\mathcal{S}_{\mathcal{D}f}$	Color coordinates domain of definition from the f function
$x = (i, j)$	Spatial coordinates for a pixel x
f^c, f^r	Complementary and reflectivity of the f function
g,$\mathcal{D}_g$	Structuring Element function and his spatial domain of definition
g', g''	Inferior and superior Structuring Element function for the $MOMP$ Transform
$h_{g'}, h_{g''}$	Value of g' and g'' function located at the spatial origin o: $g'(o) = h_{g'}$
C_x	Color coordinates of the x pixel
$\lvert\overrightarrow{C_x C_y}\rvert$	Δ_E color distance between the C_x and C_y coordinates ($\overrightarrow{C_x C_y}$ vector norm)
$O^{+\infty}, O^{-\infty}$	Color convergence coordinates for the dilation and the erosion
$\oplus_{\mathfrak{b}}, \ominus_{\mathfrak{b}}$	Dilation and erosion for binary images
$\oplus_{\mathfrak{g}}, \ominus_{\mathfrak{g}}$	Dilation and erosion for grey-level images
$\oplus_{\mathfrak{c}}, \ominus_{\mathfrak{c}}$	Dilation and erosion for color images
$\underset{\mathfrak{c}}{+}, \underset{\mathfrak{c}}{-}$	Addition and subtraction for color coordinates

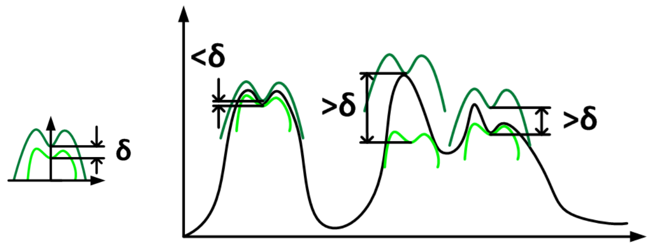

(a) SEs

(b) Probing of function

Fig. 1: Principle of the $MOMP$ transform

where $g(x)^r = g(-x)$. The result value is the distance between both SE computed at the SE origin. The shape is found when the result is lower than δ (figure 1).

This template construction with two different SE allows to extract structures with some shape and/or of contrast variations and to be few sensitive to noise in the image. To extend this construction to color, the definition of color $NFSE$ must be defined. So, the next section is dedicated to our adapted proposal for non-flat structuring elements construction.

3. COLOR MATHEMATICAL MORPHOLOGY

The most widely used methods to define minimum ($\bigvee$) and maximum ($\bigwedge$) operations in color spaces are two equivalent approaches, the *lexicographic order* or *order based on priority expressed between color axis* [12, 13, 14]. Usually, the dilation and erosion operators by the structuring element g, in n-dimensional space, can be expressed by (equations 3 and 4):

$$(f \oplus_{\mathfrak{c}} g)(i,j) = \bigvee_{(i,j)\in D_f,(k,l)\in D_g} \{f(i+k, j+l)\} \quad (3)$$

$$(f \ominus_{\mathfrak{c}} g)(i,j) = \bigwedge_{(i,j)\in D_f,(k,l)\in D_g} \{f(i+k, j+l)\} \quad (4)$$

where D_f and D_g are respectively the spatial image support and the spatial structuring element support.

Due to the natural extension from grayscale domain, and the choice of simple color order the morphological result converges towards the black or white coordinates upon the iteration scheme. As for color images the convergence coordinates could not be reduced to black or white, we propose a new method, called "Convergent Color Mathematical Morphology" ($CCMM$), to associate color morphological operators on this concept of *convergence*. Two convergence coordinates are defined according to the morphological objectives. For example, the color convergence coordinates could be associated to the color set statistics [15]. Then after an infinity number of iterations the remaining color coordinates of all pixels are the closest to the color convergence coordinate. Some authors have tried to construct a total ordering scheme integrating distance functions and the notion of reference colour [16]. But such approaches are not completely based on distance ordering. If the first condition did not reach a unique coordinate, they use a classical lexicographic construction. In addition, such approaches never define the required complementary color in terms of perception or physic property.

The basic order relation between two color coordinates is built according to the distance from the convergence color points. The convergence color points are $O^{-\infty}$ for the erosion and $O^{+\infty}$ for the dilation. Then the relations for the erosion (5) and the dilation (6) between two colors, C_1 and C_2, could be:

$$C_1 \preceq C_2 \quad \Leftrightarrow \quad |\overrightarrow{C_1 O^{-\infty}}| \leq |\overrightarrow{C_2 O^{-\infty}}| \quad (5)$$

$$C_1 \succeq C_2 \quad \Leftrightarrow \quad |\overrightarrow{C_1 O^{+\infty}}| \leq |\overrightarrow{C_2 O^{+\infty}}| \quad (6)$$

In equations (5) and (6), the vector norm $|.|$ uses the perceptual distance ΔE computed in CIELAB. In a previous work, we showed that the ΔE color distance is most accurate than the other formulations or expressions in other color spaces [17]. The (5) and (6) expressions ensure the linear convergence in a perceptual sense toward the color coordinates chosen. But they don't construct a total order as required. The complete description and the validation of a total order are not the subjects of this article, then they will not be detailed here. The definition of the maximum color coordinates on the image support $\mathcal{D}_f$ and the structuring element support $\mathcal{D}_g$, for the dilation is:

$$\bigvee_{x\in(\mathcal{D}_f\cap\mathcal{D}_g)} \{f(x)\} = \left\{C_y, C_y = \bigvee_{\forall C_x \in \mathcal{S}_{\mathcal{D}9}} \left\{C_x^{\beta}\right\}\right\} \quad (7)$$

$$\text{with} \quad \mathcal{S}_{\mathcal{D}9} = \left\{C_y : C_y = \bigvee_{\forall C_x \in \mathcal{S}_{\mathcal{D}8}} \left\{C_x^{\alpha}\right\}\right\};$$

$$\mathcal{S}_{\mathcal{D}8} = \left\{C_y : |\overrightarrow{C_y O^{-\infty}}| = \bigvee_{\forall C_x \in \mathcal{S}_{\mathcal{D}7}} \left\{|\overrightarrow{C_x O^{-\infty}}|\right\}\right\};$$

$$\mathcal{S}_{\mathcal{D}7} = \left\{C_y : |\overrightarrow{C_y C_i}| = \bigvee_{\forall C_x \in \mathcal{S}_{\mathcal{D}6}} \left\{|\overrightarrow{C_x C_i}|\right\}\right\};$$

$$\text{and} \quad \mathcal{S}_{\mathcal{D}6} = \left\{C_y : |\overrightarrow{C_y O^{+\infty}}| = \bigwedge_{\forall x \in (\mathcal{D}_f\cap\mathcal{D}_g)} \left\{|\overrightarrow{C_x O^{+\infty}}|\right\}\right\}$$

where C_x^{β} and C_x^{α} are respectively the second and the third $CIELAB$ coordinates of C_x after a translation and a rotation around the origin of the coordinates[1] and C_i is the colour at the SE coordinates origin.

3.1. Non-flat structuring element

Since there is no valid definition of addition/subtraction in color domain, we define an adapted expression to the particular case of the $CCMM$. We impose that color pixel displacement stills in relation with the notion of *convergence*. Color addition ($\underset{\mathfrak{c}}{+}$)/subtraction ($\underset{\mathfrak{c}}{-}$) induces the displacement of the

[1] In order to the theoretical validation of the duality property.

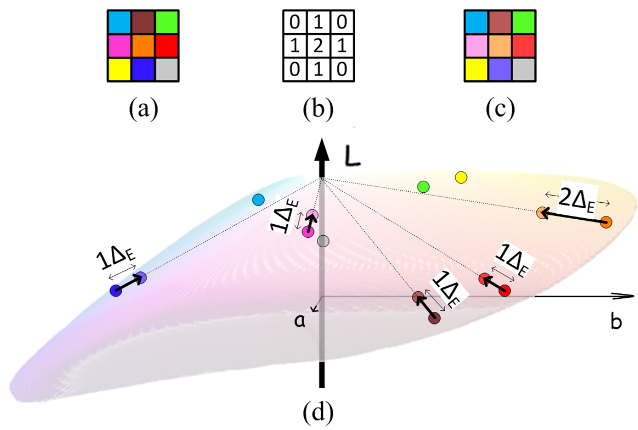

Fig. 2: Example of vector displacements with color addition ($\underset{c}{+}$), the convergence color is the white and the divergence color is the black; (a) Original set of colors; (b) Non-flat structuring element; (c) New set of colors; (d) Calculation of new coordinates of the set of colors

pixels in the color space. The color vector displacement is defined by its magnitude and its orientation. Dealing with color representation, we associate the magnitude to specific color metric and we propose to use Δ_E metric. The orientation depends on the morphological operation: with addition the displacement is oriented toward convergence color coordinates. On the contrary, with subtraction, the displacement is oriented toward divergence coordinates. The figure 2 shows an example of color displacements in addition case.
Then the color $MOMP$ ($CMOMP$) is naturally written:

$$CMOMP_g(f)(x) = \Delta_E \left(\bigvee_{(i,j)\in\mathcal{D}_f,(k,l)\in\mathcal{D}_g} \{f(i+k,j+l) \underset{c}{-} g(k,l)\} \; , \bigwedge_{(i,j)\in\mathcal{D}_f,(k,l)\in\mathcal{D}_g} \{f(i+k,j+l) \underset{c}{-} g(-k,-l)\} \right) \quad (8)$$

4. THEORETICAL RESULTS

The Hit-or-Miss Transform was developed to allow the extraction of particular shapes from images. The first experimentation evaluates this ability on synthetical color images. We focus the experimentation on the color accuracy of the shape extraction. The searched shapes are color crosses of size 5 by 5 pixels, with different filling colors and color background. The structuring elements used to extract crosses are designed with contrast equal to δ ($\delta = h_{g''} - h_{g'}$) (figure 3). In this paper, all the images are constructed in the RGB space and the $CMOMP$ is performed in the $CIELAB$ space.

In this part we search to determine the capability of the $CMOMP$ to detect shapes of particular color. For this experiment, different color crosses are drawn on a uniform black background (figure 4-(a)). And we experiment the extraction of particular color crosses: the red ones, the green and the blue ones. The $CMOMP$ is applied using adapted convergence color: the convergence point of the erosion is the background color and that of the dilation is the color of searched crosses.

In an other work, we have established[2] the relation between the grayscale or color contrast selectivity and the maximum values of the non flat structuring elements. In figure 4, we illustrate this color selectivity impact in front of the convergence color coordinates choices (selectivity level). We set the selectivity parameter at the same value for the three results with different convergence coordinates. And the selectivity parameter is defined with a middle range. The found color crosses are in accordance with the searched color and valid our approach operation.

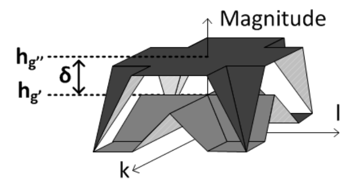

Fig. 3: 3D view of the template

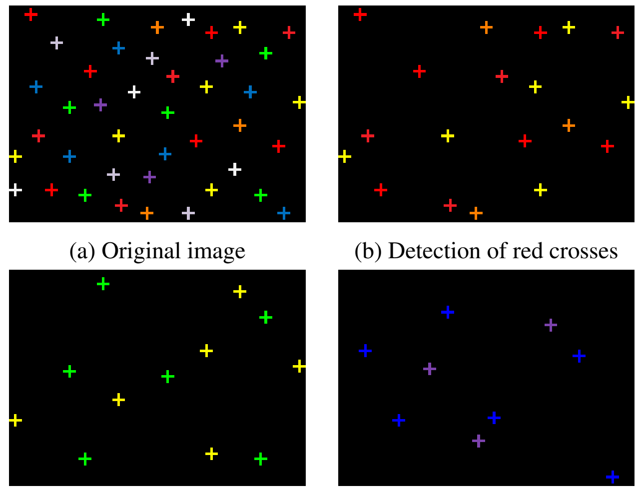

(a) Original image (b) Detection of red crosses

(c) Detection of green crosses (d) Detection of blue crosses

Fig. 4: Detection of crosses (size : 5x5) on black background

5. RESULTS ON SKIN IMAGES

5.1. The experiment

Skin images are very complex color images, with lot of diffuse color information, lot of variations in the color back-

[2]Submitted article.

ground or skin artifacts or diseases depending of the human diversity of origin and life conditions. Classical ways or image processing fails to solve robust images processing routines due to this diversity, and to the fact that these images are analyzed by human expert with a non linear perception and not by computer system. So it exists a great necessity to produce color image processing systems in accordance to the Human Visual System, to be in agreement with the experts.

The aim of this experimental part is to find rosacea in a skin image. For this first evaluation, we work on some images valuated by the expert in function of rosacea level. The major difficulty of this evaluation is induced by the very low contrast of rosacea in a skin image, in particular for the images valuated as low rank. Moreover, the color of the rosacea is close to the skin color. Rosacea are defined by a sequence of connected linear segment with color close to the hemoglobin one. The more adapted shape is a line extraction. The contrast and/or the width of the rosacea is function of severity level. Then the g'' is wider and higher than the g' to allow these variations. Moreover, as the rosacea have different orientations, we apply these structuring elements in 8 directions. The final result is the union of the $CMOMP$ result with this different orientations. Next, the chosen convergence colors are the skin background for the erosion ($O^{-\infty}$) and the rosacea color for the dilation ($O^{+\infty}$). At this level, these colors are defined in a supervised way, in others works we used a statistical processing to identify the right color convergence coordinates. The $h_{g''}$ and $h_{g'}$ values are manually set.

5.2. Discussion

Some results of the $CMOMP$ algorithm are shown in figures 5 to 8. The figures show the initial image (a) and the direct result of the $CMOMP$ (b). The principal searched structures are well detected. And, in front of the severity level ranked by the expert, the amount of kept pixels is perfectly correlated (table 2). But as no ground truth exists for these images, it is not possible to establish an accuracy criterion or adjust the selectivity parameter. Then, we develop a dedicated database to assess our approach. Different kinds of variations are in course for diffuse objects extraction in skin images, or for complex artifacts like those induced by psoriasis. But the major work lies in the extension of this purpose in a multi-scale approach.

6. CONCLUSION

In this paper, we presented our definition for a color mathematical morphology based on the concept of *convergence*. This new approach allows the extension of color mathematical morphology to Non-Flat Structuring Element, that had never been defined before. The originality of the expression is to solve the problem of the addition/subtraction definition in color domain. This definition uses the particularity of the

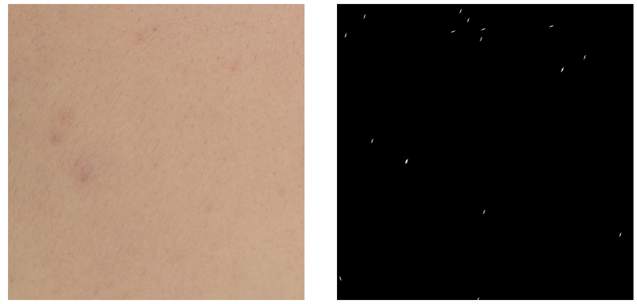

(a) Original image (b) $CMOMP$ results

Fig. 5: Image of skin with rosacea (intensity = 0)

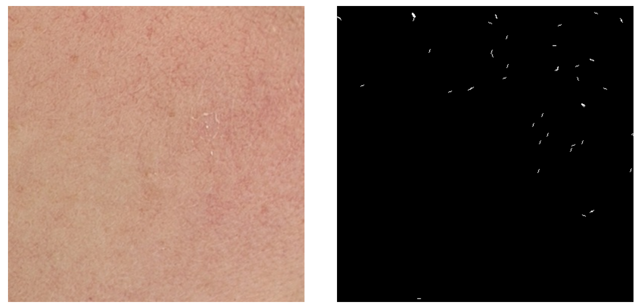

(a) Original image (b) $CMOMP$ results

Fig. 6: Image of skin with rosacea (intensity = 1)

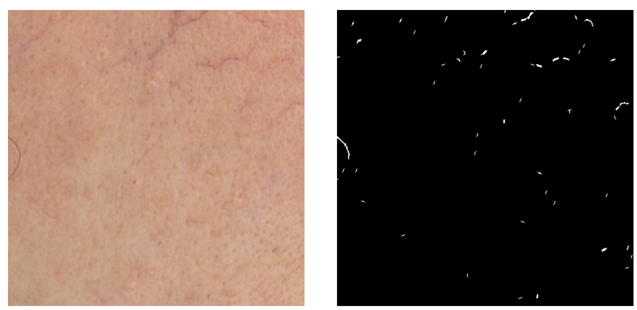

(a) Original image (b) $CMOMP$ results

Fig. 7: Image of skin with rosacea (intensity = 2)

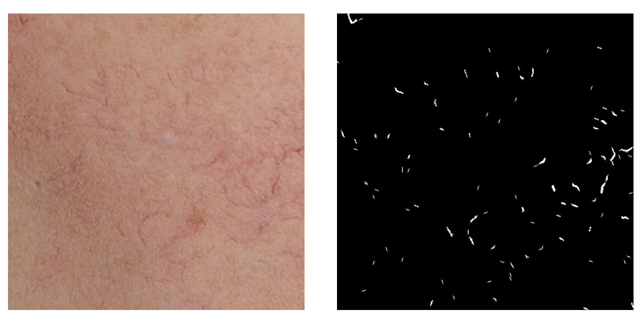

(a) Original image (b) $CMOMP$ results

Fig. 8: Image of skin with rosacea (intensity = 3)

Table 2: Number of extracted pixels in each result images

	$CMOMP$ result
figure 5-(b) (severity = 0)	10
figure 6-(b) (severity = 1)	233
figure 7-(b) (severity = 2)	518
figure 8-(b) (severity = 3)	1073

color convergence and a normalized color distance function. Consequently, the complete color mathematical morphological expression is valid in the sense of color distances standardized by the CIE. Thanks to this possibility, we extended the Hit-or-Miss Transform defined by Barat to the color domain. The major interest of this method is to allow template construction for color shape extraction in images. Then we shown on synthetic images the capabilities of color selectivity obtained by our color Hit-or-Miss Transform. In particular by using a color distance function as the ΔE metric, expressed in CIELAB. This metric allows extracting color shapes in correlation with the Human Visual System perception.

The Color Hit-or-Miss Transform was applied on skin images to detect specific lesions, the rosacea. The first obtained results shows that the total area of rosacea extracted by the Hit-or-Miss transform is correlated with the score given by the expert. These results are very encouraging, and we work now to better define the structuring element used in the transform and the cooperation between different transformations to enhance the capabilities to extract complex color shapes in dermatology.

Acknowledgment

This work is a part of a project MORFISM supported by L'Oréal and a project agreements State-region (EDRF).

7. REFERENCES

[1] L. Busin, N. Vandenbroucke, and L. Macaire, *volume 151 of Advances in Imaging and Electron Physics*, chapter Chapter 2 : Color spaces and image segmentation, pp. 65–168, Elsevier Inc., 2008.

[2] V. Barnett, "The ordering of multivariate data," *Journal of the Royal Statistical Society. Series A (General)*, pp. 318–355, 1976.

[3] E. Aptoula and S. Lefèvre, "A comparative study on multivariate mathematical morphology," *Pattern Recognition*, vol. 40, no. 11, pp. 2914–2929, 2007.

[4] P. Maragos and R. Schafer, "Morphological filters–part i: Their set-theoretic analysis and relations to linear shift-invariant filters," *Acoustics, Speech and Signal Processing, IEEE Transactions on*, vol. 35, no. 8, pp. 1153–1169, 1987.

[5] S. Peleg, J. Naor, R. Hartley, and D. Avnir, "Multiple resolution texture analysis and classification," *Pattern Analysis and Machine Intelligence, IEEE Transactions on*, , no. 4, pp. 518–523, 1984.

[6] C. Barat, C. Ducottet, et al., "Pattern matching using morphological probing," in *Image Processing, ICIP. Proceedings. International Conference on*. IEEE, 2003, vol. 1, pp. I–369.

[7] J. Serra, *Image Analysis and Mathematical Morphology*, vol. I, Academic Press, 1982.

[8] E.R. Dougherty, "Optimal mean-absolute-error filtering of gray-scale signals by the morphological hit-or-miss transform," *Journal of Mathematical Imaging and Vision*, vol. 4, no. 3, pp. 255–271, 1994.

[9] M. Khosravi and R.W. Schafer, "Template matching based on a grayscale hit-or-miss transform," *Image Processing, IEEE Transactions on*, vol. 5, no. 6, pp. 1060–1066, 1996.

[10] P. Soille, "Advances in the analysis of topographic features on discrete images," in *Discrete Geometry for Computer Imagery*. Springer, 2002, pp. 271–296.

[11] B. Naegel, N. Passat, and C. Ronse, "Grey-level hit-or-miss transforms–part i: Unified theory," *Pattern Recognition*, vol. 40, no. 2, pp. 635–647, 2007.

[12] G. Louverdis, MI Vardavoulia, I. Andreadis, and P. Tsalides, "A new approach to morphological color image processing," *Pattern recognition*, vol. 35, no. 8, pp. 1733–1741, 2002.

[13] A. Hanbury and J. Serra, "Mathematical morphology in the hls colour space," in *12th British Machine Vision Conference, Manchester, UK*. Citeseer, 2001, pp. 451–460.

[14] J. Angulo and J. Serra, "Morphological coding of color images by vector connected filters," in *Signal Processing and Its Applications (7th International Symposium on)*. IEEE, 2003, vol. 1, pp. 69–72.

[15] M. Ivanovici, A. Caliman, N. Richard, and C. Fernandez-Maloigne, "Towards a multivariate probabilistic morphology for colour images," 2012.

[16] J. Angulo, "Morphological colour operators in totally ordered lattices based on distances: Application to image filtering, enhancement and analysis," *Computer Vision and Image Understanding*, vol. 107, no. 1-2, pp. 56–73, 2007.

[17] A. Ledoux, N. Richard, A.S. Capelle-Laizé, et al., "Limitations et comparaisons d'ordonnancement utilisant des distances couleur," 2011.